2023 62nd IEEE Conference on Decision and Control (CDC)
December 13-15, 2023. Marina Bay Sands, Singapore

Convexification of Robust Trajectory Planning Problems With Nominal State and Control Dependent Uncertainties

Oliver Sheridan Behçet Açıkmeşe

Abstract— **We consider the problem of robust trajectory optimization of constrained discrete-time linear systems under bounded uncertainty. This paper extends our previous work on robust trajectory planning for linear systems with control-dependent uncertainties to a more general class of uncertainties, including nominal-state-dependent uncertainties. In particular, we show that if strong duality holds for the robust state constraints, and if the uncertainties are bounded by convex elementwise nonnegative functions of the nominal state and control, the robust constraints can be equivalently reformulated as deterministic convex constraints, enabling globally optimal solutions with no conservatism. We first use convex duality theory to reformulate robust linear inequality state constraints as deterministic biconvex constraints . We then exploit the elementwise nonnegativity of the uncertainty bounds to remove the biconvexity in closed form, resulting in convex deterministic constraints that can be handled by off-the-shelf solvers. These two lemmas are our main contribution, and lead to our final result, and equivalent convex reformulation of the original robust optimization problem which allows efficient trajectory optimization solutions under control and state dependent uncertainties. We then demonstrate the practical applicability of our method via numerical simulations.**

I. Introduction

This paper describes a key useful generalization of our previous work [1] on robust trajectory optimization of discrete-time linear dynamical systems. As in that paper, we consider discrete-time linear dynamical systems subject to linear inequality constraints on the state, which must be satisfied robustly for any realization of a perturbation which, while unknown, is assumed to lie in a known set at each time step. Our principal motivating real-world example is optimal trajectory planning for orbital spacecraft rendezvous. For such trajectory planning problems, the presence of uncertainty in the dynamics has important performance and safety implications. In [1], we described a method of generating robust linearly-constrained trajectories subject to control-dependent perturbations; this allowed us to incorporate the common Gates maneuver error model [2] into a deterministic convex optimization framework. Navigation uncertainty can also create apparent dynamic disturbances: if the true state of the vehicle is different from the measured state, the actual evolution of the state will not match what we predict from the measured state. Autonomous vehicles often make use of relative navigation techniques such as lidar [3] and optical computer vision algorithms [4]. The navigation errors these produce are often dependent on the vehicle state. For example, vision-based systems require illumination of the target, so that a chaser vehicle approaching from the dark side of a target vehicle may have worse state estimates than one approaching from the sunlit side; the performance of lidar can be degraded by varying reflectivity on different parts of the target vehicle; etc.. Thus, practical trajectory-optimization techniques for spacecraft rendezvous should ideally be able to handle state-dependent uncertainties. State-dependent disturbances are also relevant outside the domain of spacecraft trajectory planning; for example, aerodynamic force disturbances on aircraft are often dependent on dynamic pressure, which is a function of airspeed. In this paper, we extend our method to not only handle more general control-dependent uncertainties, but to also handle state-dependent uncertainties in a unified solution approach.

There are two broadly-prevailing methods for dealing with uncertainty in trajectory planning [5]: the stochastic approach, in which perturbations (and hence the state) are modeled as random variables with known probability distributions, and all constraints are converted to chance constraints; and the "robust" approach, in which it is assumed that all possible perturbations lie in known sets, and trajectories are planned which remain feasible for any realization of the perturbations. We use the latter approach in this paper.

In the literature, uncertainties in the dynamics (and hence in the state after any amount of propagation) are often handled by simply applying buffered constraints to the nominal trajectory, resulting in the nominal trajectory standing off some distance from the desired boundary [6], [7], [8]. These constraint buffers are often conservative, being computed with heuristics or overapproximations of the true uncertainty sets. Model-predictive control (MPC) is a popular approach to handling state-dependent uncertainties in particular [9], [10], [11]. This is again often accomplished by simplifying the uncertainty sets to more tractable overapproximations, thus introducing conservatism to the final trajectories. While the method we present also essentially works by buffering the state constraints, our method results in an exactly-equivalent deterministic reformulation of the original robust constraint: if strong duality holds for the original robust constraint, our method results in a zero-conservatism equivalent deterministic problem.

This work is supported by National Science Foundation grant CMMI-2105631, Air Force Office of Scientific Research grant FA9550-20-1-0053, Office of Naval Research grant ONR N00014-20-1-2288, and Blue Origin, LLC.

Oliver Sheridan is a research assistant at the Department of Aeronautics & Astronautics, University of Washington, Seattle, WA 98195-2400, USA westward@uw.edu

Behçet Açıkmeşe is with the faculty of the Department of Aeronautics & Astronautics, University of Washington, Seattle, WA 98195-2400, USA behcet@uw.edu

A. Notation

In the following sections, lowercase variables represent vectors, and uppercase variables represent matrices. $\mathbf{R}^n$ is the set of real vectors of dimension n, $\mathbf{R}^{m\times n}$ is the set of real m-by-n matrices, and e_i is the i-th standard basis vector (i.e., the i-th element of e_i is one, and all others are zero). The symbols $\preceq$ and $\succeq$ represent elementwise vector and matrix inequalities, and the symbols $\leq$ and $\geq$ represent scalar inequalities. The function $\max(A, B)$ is the elementwise maximum of A and B, and $\min(A, B)$ is the elementwise minimum. $\mathbf{I}_{n\times n}$ is the n-by-n identity matrix, and $\mathbf{0}_{m\times n}$ and $\mathbf{1}_{m\times n}$ are m-by-n matrices of zeros and ones, respectively. The constant matrix $\mathcal{C}_1$ is $\mathcal{C}_1 = \begin{bmatrix}1 & -1\end{bmatrix}$, and the matrix $\mathcal{C}_n$ is

$$\mathcal{C}_n = \mathbf{I}_{n\times n} \otimes \mathcal{C}_1,$$

where $\otimes$ is the Kronecker product. for example:

$$\mathcal{C}_2 = \begin{bmatrix}1 & -1 & 0 & 0\\ 0 & 0 & 1 & -1\end{bmatrix}.$$

The notation $(A)_{ij}$ denotes the element of A in the i-th row and j-th column; for vectors, the notation $(a)_i$ denotes the i-th element.

II. Problem Formulation

We consider a discrete-time linear time-varying system with state x, nominal control input u, external environmental input v, perturbation w on the external input, and an additional state- and control-dependent perturbation n. Thus for any time $t = 1, 2, ...,$

$$x_{t+1} = A_t x_t + B_t u_t + E_t(v_t + w_t) + K_t n_t.$$

The external input terms v and w are included for generality; in the case of spacecraft trajectory planning, this external input might represent solar radiation pressure or aerodynamic drag, for example. The separate perturbation n is assumed to be dependent on the nominal state and control, and must therefore be handled separately from the state- and control-independent term w.

In the following sections we work with a stacked-variable formulation of this problem, with the stacked matrices $\bar{A}_t$, $\bar{B}_t$, $\bar{E}_t$, and $\bar{K}_t$ defined as:

$$\begin{aligned}
\bar{A}_t &= A_t A_{t-1} ... A_0\\
\bar{B}_t &= \begin{bmatrix}A_t A_{t-1} ... A_1 B_0 & A_t A_{t-1} ... A_2 B_1 & \cdots & B_t\end{bmatrix}\\
\bar{E}_t &= \begin{bmatrix}A_t A_{t-1} ... A_1 E_0 & A_t A_{t-1} ... A_2 E_1 & \cdots & E_t\end{bmatrix}\\
\bar{K}_t &= \begin{bmatrix}A_t A_{t-1} ... A_1 K_0 & A_t A_{t-1} ... A_2 K_1 & \cdots & K_t\end{bmatrix}.
\end{aligned}$$

For any vector variable a_t, the stacked form is defined as: $\bar{a}_t = \begin{bmatrix}a_0^T & a_1^T & \cdots & a_t^T\end{bmatrix}^T$. Note then that for any time $t = 1, 2, ...,$

$$x_t = \bar{A}_{t-1} x_0 + \bar{B}_{t-1}\bar{u}_{t-1} + \bar{E}_{t-1}(\bar{v}_{t-1} + \bar{w}_{t-1}) + \bar{K}_{t-1}\bar{n}_{t-1}.$$

In the following, we also consider state propagation due to nominal inputs, and define the following *nominal system dynamics*

$$x_t^n = \bar{A}_{t-1} x_0 + \bar{B}_{t-1}\bar{u}_{t-1} + \bar{E}_{t-1}\bar{v}_{t-1} \tag{1}$$

and the deviation from the nominal state is captured by

$$\Delta x_t = \bar{K}_{t-1}\bar{n}_{t-1} + \bar{E}_{t-1}\bar{w}_{t-1}. \tag{2}$$

Note that $x_t = x_t^n + \Delta x_t$.

In this paper, we impose a linear inequality constraint $H_t x_t \preceq h_t$, where $H_t \in \mathbf{R}^{m_t\times n_x}$, $h_t \in \mathbf{R}^{m_t}$. Since x_t depends on the unknown but bounded disturbances w_t and n_t, we wish to apply this constraint robustly, so that it is satisfied for any realization of w_t and n_t; thus we must assume some known sets in which these perturbations lie.

For the state and control dependent uncertainty n_t, we make the following assumption:

Assumption 1. *$0 \preceq n_t \preceq f(x_t^n, u_t)$, where the function f is convex and elementwise nonnegative for all x_t^n and u_t.*

The above assumption bounds the set of possible uncertainties as a function of the nominal state and control. Hence the choice of the nominal state and control trajectories implies a choice of uncertainties to be experienced by the dynamics. As shown in [1], this uncertainty characterization is used in spacecraft control problems for control dependent uncertainties, via the Gates model [2].

Finally, for our uncertainty model we must assume known bounds on the exogenous input uncertainty w_t. In this case we simply assume that the set of possible disturbances at each time step is a known polytope:

Assumption 2. *The external input perturbation w_t is constrained to a polytope $G_t w_t \preceq g_t$.*

To express our uncertainty bounds in stacked form, we define:

$$\bar{G}_t = \begin{bmatrix}G_0 & & & \\ & G_1 & & \\ & & \ddots & \\ & & & G_t\end{bmatrix},$$

$$\bar{f}_t(\bar{x}_t^n, \bar{u}_t) = \begin{bmatrix}f(x_0^n, u_0)\\ f(x_1^n, u_1)\\ \vdots \\ f(x_t^n, u_t)\end{bmatrix}.$$

Then, an optimal control problem with cost function $J(\bar{x}_N^n, \bar{u}_{N-1})$ over time horizon $t \in \{1, 2, \ldots, N\}$ under the above assumptions, and subject to polytopic state constraints, is formulated as follows:

$$\begin{aligned}
&\underset{\bar{x}_N^n,\, \bar{u}_{N-1}}{\text{minimize}} \quad J(\bar{x}_N^n, \bar{u}_{N-1}) && \text{(3a)}\\
&\text{subject to}\\
&x_t = x_t^n + \Delta x_t \text{ satisfying eqs.(1), (2)} \quad t = 1, \ldots, N, && \text{(3b)}\\
&H_t x_t \preceq h_t \quad \forall (\bar{w}_{t-1}, \bar{n}_{t-1}) \in \bar{\mathbf{P}}_{t-1} \quad t = 1, \ldots, N && \text{(3c)}
\end{aligned}$$

where

$$\bar{\mathbf{P}}_k = \{(\omega, \nu) \mid \bar{G}_k \omega \preceq \bar{g}_k,\ 0 \preceq \nu \preceq \bar{f}(\bar{x}_k^n, \bar{u}_k)\}.$$

In the following section we develop an equivalent dual formulation of constraint (3c), and corresponding convex representation of this robust optimization problem.

III. Lossless Convexification of Robust State Constraints

Inspection of the constraint (3c) reveals that it can also be expressed as follows:

$$\max_{(\bar{w}_{t-1},\bar{n}_{t-1})\in\bar{\mathbf{P}}_{t-1}} e_i^T H_t x_t \le e_i^T h_t, \quad i=1,\dots,m_t. \tag{4}$$

Thus constraint (3c) is itself really a statement about the optimal values of a collection of subsidiary maximization problems. However, we can exploit the duality theory of convex optimization to find upper bounds to these maximization problems, and thus reduce our constraint to a set of tractable, deterministic convex constraints.

The dual of a maximization problem is a minimization problem, and any feasible cost of this dual minimization problem is an upper bound on the primal maximization problem [12]. Since upper bounds on the problems (4) are what we desire for robust constraint satisfaction, re-expressing this constraint in dual form provides a useful technique to simplify our analysis. Similar duality-based techniques have been utilized in set-based analysis of control systems [13], [14], specifically for establishing invariant sets for control systems [15], [16] and Markov chains [17], [18]. The transformation of our robust linear state constraint to a set of deterministic convex constraints relies on the following lemma.

Lemma 1. *If strong duality holds for the problems* (4)*, the robust state constraint* (3c) *is equivalent to the following: there exist elementwise nonnegative matrices Z_t and Λ_t such that:*

$$Z_t\bar{G}_{t-1} = H_t\bar{E}_{t-1} \tag{5a}$$

$$\Lambda_t \succeq H_t\bar{K}_{t-1} \tag{5b}$$

$$\underbrace{Z_t\bar{g}_{t-1} + \Lambda_t\bar{f}(\bar{x}_{t-1}^n,\bar{u}_{t-1})}_{\textit{uncertainty buffer}} \preceq \underbrace{h_t - H_t x_t^n}_{\textit{nominal state constraint}}. \tag{5c}$$

Proof. We bound the problems (4) above through duality. To form the dual of problems (4), we first transform them into a more convenient form. Through some straightforward algebra, we can see that

$$\begin{aligned}
&\max_{(\bar{w}_{t-1},\bar{n}_{t-1})\in\bar{\mathbf{P}}_{t-1}} e_i^T H_t x_t \le e_i^T h_t \\
\equiv &\max_{(\bar{w}_{t-1},\bar{n}_{t-1})\in\bar{\mathbf{P}}_{t-1}} e_i^T H_t\left(x_t^n + \Delta x_t\right) \le e_i^T h_t \\
\equiv &\max_{(\bar{w}_{t-1},\bar{n}_{t-1})\in\bar{\mathbf{P}}_{t-1}} e_i^T H_t\Delta x_t \le e_i^T\left(h_t - H_t x_t^n\right).
\end{aligned}$$

Expanding Δx_t and re-expressing the constraints on $(\bar{n}_{t-1},\bar{w}_{t-1})$, we arrive at the following equivalent formulation of (3c):

$$\begin{aligned}
\max_{\bar{w}_{t-1},\bar{n}_{t-1}} \; & e_i^T H_t\left(\bar{K}_{t-1}\bar{n}_{t-1} + \bar{E}_{t-1}\bar{w}_{t-1}\right) \le e_i^T\left(h_t - H_t x_t^n\right) \\
\text{s.t. } & 0 \preceq \bar{n}_{t-1} \preceq \bar{f}(\bar{x}_{t-1}^n,\bar{u}_{t-1}), \\
& \bar{G}_{t-1}\bar{w}_{t-1} \preceq \bar{g}_{t-1}.
\end{aligned}$$

The dual of this problem is:

$$\begin{aligned}
\min_{\lambda_i,z_i} \; & \lambda_i^T\bar{f}(\bar{x}_{t-1}^n,\bar{u}_{t-1}) + z_i^T\bar{g}_{t-1} \\
\text{s.t. } & \lambda_i \succeq 0,\ \lambda_i \succeq e_i^T H\bar{K}_{t-1},\ z_i \succeq 0, \\
& z_i^T\bar{G}_{t-1} = e_i^T H_t\bar{E}_{t-1}.
\end{aligned}$$

Since, as stated before, any dual-feasible cost provides an upper bound on the primal problem, then if strong duality holds (and the duality gap at optimality is zero) our constraint is equivalent to the following:

$$\text{for } i=1,\dots,m_t, \quad \exists\lambda_i \succeq 0,\ z_i \succeq 0$$

such that

$$\begin{aligned}
\lambda_i &\succeq e_i^T H\bar{K}_{t-1} \\
z_i^T\bar{G}_{t-1} &= e_i^T H_t\bar{E}_{t-1} \\
z_i^T\bar{g}_{t-1} + \lambda_i^T\bar{f}(\bar{x}_{t-1}^n,\bar{u}_{t-1}) &\preceq e_i^T\left(h_t - H_t x_t^n\right).
\end{aligned}$$

Thus, stacking the i-dependent variables into the matrices $Z_t = \begin{bmatrix} z_1 & \dots & z_{m_t}\end{bmatrix}^T$ and $\Lambda_t = \begin{bmatrix}\lambda_1 & \dots & \lambda_{m_t}\end{bmatrix}^T$, we arrive at the conclusions of the lemma. □

The constraints of Lemma 1 are almost convex, but not quite: constraint (5c) is biconvex, since Λ_t, $\bar{x}_{t-1}^n$, and $\bar{u}_{t-1}$ are decision variables. However, we note the following:

Remark 1. *If the left-hand-side (LHS) of constraint* (5c) *is zero, this corresponds to the zero-uncertainty polytopic state constraint. Any positive value of the LHS enforces an uncertainty buffer holding the nominal trajectory away from the polytopic constraint. Therefore we can minimize conservatism by elementwise minimizing the LHS of* (5c)*.*

Also note that the biconvex terms in the LHS of constraint (5c) are elementwise nonnegative. Therefore we can minimize the biconvex contribution to the uncertainty buffer by minimizing Λ_t elementwise, leading to the following lemma.

Lemma 2. *The biconvex term $\Lambda_t\bar{f}(\bar{x}_{t-1}^n,\bar{u}_{t-1})$ in constraint* (5c) *can be equivalently replaced by the term $\Gamma_t\bar{f}(\bar{x}_{t-1}^n,\bar{u}_{t-1})$, where $\Gamma_t = \max\left(0, H_t\bar{K}_{t-1}\right)$.*

Proof. Since $\Lambda_t\bar{f}(\bar{x}_{t-1}^n,\bar{u}_{t-1})$ is convex separately in Λ_t, $\bar{x}_{t-1}$, and $\bar{u}_{t-1}$, the minimum of this term can be found by minimizing over each variable separately in succession. Since Λ_t, and $\bar{f}(\bar{x}_{t-1}^n,\bar{u}_{t-1})$ are both elementwise nonnegative, we can minimize over Λ_t in closed form by simply minimizing Λ_t elementwise. If any particular element $(H_t\bar{K}_{t-1})_{ij}$ is nonnegative, then if we simply take the corresponding element $(\Lambda_t)_{ij}$ to be equal to $(H_t\bar{K}_{t-1})_{ij}$ then we have minimized that element $(\Lambda_t)_{ij}$ according to constraint (5b).

If on the other hand a particular element $(H_t\bar{K}_{t-1})_{ij}$ is negative, then we cannot take the corresponding element of $(\Lambda_t)_{ij}$ to equal $(H_t\bar{K}_{t-1})_{ij}$, since Λ_t must be elementwise nonnegative. In this case the minimum feasible value of $(\Lambda_t)_{ij}$ is zero.

Careful inspection reveals that these optimal assignments are equivalently expressed as $\Lambda_t^* = \max\left(0, H_t\bar{K}_{t-1}\right)$. Defining $\Gamma_t = \Lambda_t^*$ completes the proof. □

Combining Lemmas 1 and 2 leads immediately to the following theorem, which is the main technical result of this paper.

Theorem 1. *If strong duality holds for the problems* (4)*, the robust state constraint* (3c) *is equivalent to the following:*

$$\begin{aligned} Z_t &\succeq 0, \\ Z_t \bar{G}_{t-1} &= H_t \bar{E}_{t-1}, \\ Z_t \bar{g}_{t-1} + \Gamma_t \bar{f}(\bar{x}^n_{t-1}, \bar{u}_{t-1}) &\preceq h_t - H_t x^n_t, \end{aligned}$$

where

$$\Gamma_t = \max\left(0, H_t \bar{K}_{t-1}\right).$$

And thus we have rendered the robust state constraint (3c) suitable for convex programming methods. Our final problem formulation is thus:

$$\begin{aligned} &\underset{\bar{x}^n_N,\, \bar{u}_{N-1}}{\text{minimize}} \quad J(\bar{x}^n_N, \bar{u}_{N-1}) && \text{(6a)} \\ &\text{subject to} \\ &Z_t \bar{G}_{t-1} = H_t \bar{E}_{t-1}, \quad Z_t \succeq 0, && \text{(6b)} \\ &x^n_t = \bar{A}_{t-1} x_0 + \bar{B}_{t-1} \bar{u}_{t-1} + \bar{E}_{t-1} \bar{v}_{t-1} \quad t = 1, \ldots, N, && \text{(6c)} \\ &Z_t \bar{g}_{t-1} + \Gamma_t \bar{f}(\bar{x}^n_{t-1}, \bar{u}_{t-1}) \preceq h_t - H_t x^n_t && \text{(6d)} \end{aligned}$$

where

$$\Gamma_t = \max\left(0, H_t \bar{K}_{t-1}\right).$$

Remark 2. *The constraints of problem* (6) *are convex, i.e., the original robust trajectory planning problem is convexified losslessly. Thus, the resulting optimization problem can be solved to global optimality by a wide range of fast and reliable interior-point-method (IPM) and first-order gradient descent solvers for convex optimization such as MOSEK [19], ECOS [20], and the proportional-integral projected gradient (PIPG) method [21].*

IV. Numerical Examples

We now show some example simulations. We start with a simple two-dimensional double integrator toy problem to demonstrate the basic functionality of the algorithm, and then we show a problem with more complicated dynamics and constraints, more reminiscent of a practical orbital rendezvous problem. In both examples the dynamics are first defined in continuous time; both are then discretized by assuming piecewise-constant control and external inputs between discretization points; i.e., we discretize with zeroth-order hold [22].

A. Double Integrator Example

We start with continuous-time two-dimensional double integrator dynamics (neglecting exogenous input and uncertainty in this case for convenience) with state $x = \begin{bmatrix} r_x & r_y & \dot{r}_x & \dot{r}_y \end{bmatrix}^T$ (position components r_x, r_y have units of meters, velocity components $\dot{r}_x$, $\dot{r}_y$ have units of m/s), and control $u = \begin{bmatrix} a_x & a_y \end{bmatrix}^T$ (units of $\mathrm{m/s^2}$). This models a point mass moving on a frictionless plane under the influence of the force vector u. Our full continuous-time dynamics are:

$$\dot{x} = \begin{bmatrix} \mathbf{0}_{2\times2} & \mathbf{I}_{2\times2} \\ \mathbf{0}_{2\times2} & \mathbf{0}_{2\times2} \end{bmatrix} x + \begin{bmatrix} \mathbf{0}_{2\times2} \\ \mathbf{I}_{2\times2} \end{bmatrix} u + \begin{bmatrix} K_x & K_u \end{bmatrix} \begin{bmatrix} n_x \\ n_u \end{bmatrix}$$

where

$$K_x = \begin{bmatrix} 0.1 \times \mathcal{C}_2 & \mathbf{0}_{2\times4} \\ \mathbf{0}_{2\times4} & 0.01 \times \mathcal{C}_2 \end{bmatrix}, \quad K_u = \begin{bmatrix} \mathbf{0}_{2\times4} \\ \mathcal{C}_2 \end{bmatrix}.$$

For the uncertainty bounds, we assume the following:

$$0 \preceq \begin{bmatrix} n_x \\ n_u \end{bmatrix} \preceq \begin{bmatrix} 5 \times f_x(x,u) \\ 0.1 \times f_u(x,u) \end{bmatrix} \tag{7}$$

where

$$\begin{aligned} f_x(x,u) &= \mathbf{1}_{8\times1} \times |r_y|, \\ f_u(x,u) &= \begin{bmatrix} \mathbf{1}_{2\times1} \times |a_x| \\ \mathbf{1}_{2\times1} \times |a_y| \end{bmatrix}. \end{aligned}$$

The coefficients 5 and 0.1 in equation (7) are simply relative weighting parameters we used to tune this particular toy problem; they have no analytical significance.

The structure and meaning of the matrices K_x and K_u bear some explanation. Note that by Assumption 1, the perturbation n is elementwise nonnegative. If we wish to model real-world perturbations n^{true} which cannot be guaranteed to be nonnegative, this can be done by representing each element $(n^{true})_i$ by a pair of elements in n: one equal to $\max(0, (n^{true})_i)$ and one equal to $-\min(0, (n^{true})_i)$. Both of these elements of n are nonnegative, and by taking their difference we can recover the entire range of the element $(n^{true})_i$. Thus, observe that the first row of K_x (for example) has the effect of creating from the nonnegative first two elements of n_x a single "effective" perturbation component (possibly negative) on the state r_x, and similarly for the other rows.

The perturbation term $K_x n_x$, when coupled with the uncertainty constraint function $f_x(x,u)$, represents position and velocity uncertainty terms that are dependent on the absolute value of the r_y position component. In other words, the farther our point mass is from the r_x axis, the greater the state uncertainty. The perturbation term $K_u n_u$, when coupled with the uncertainty constraint function $f_u(x,u)$, represents control uncertainty: an additional unknown control term which is bounded by a function of the nominal control. These control perturbation components are bounded proportionally to the absolute value of the nominal control components: the larger the nominal control, the larger the uncertainty on it. For spacecraft maneuver planning, this is a reasonable assumption in many cases; see for example [2] for a similar model.

In addition to the above dynamics, we impose the following constraints: initial state at the origin, final position in $r_x \in [2,3]$, $r_y \in [1,2]$, and final velocity in [-0.5, 0.5] in both components. Note that we cannot constrain the final state to a single point in the state space, due to the uncertainty in the dynamics; exact equality constraints cannot be satisfied robustly with nonzero uncertainty. Thus we impose the final state box constraint as above.

Discretizing the continuous-time dynamics with zeroth-order hold (20 discretization points, 0.1 second apart), we then implement a minimum-control-effort trajectory optimization problem in the Python programming language using `cvxpy` [23] as a parsing layer, with ECOS [20] as the underlying numerical solver. We compute three trajectories for illustration: one with no uncertainty, one with only control-dependent uncertainty, and one with both state- and

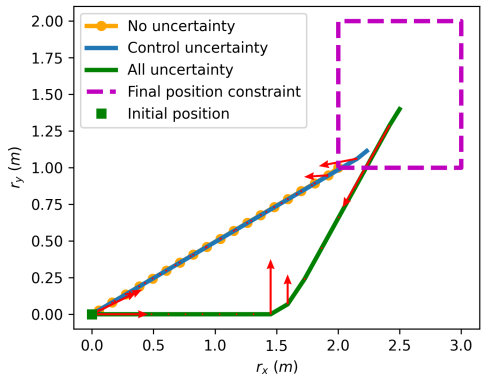

Fig. 1: Double integrator nominal trajectories.

control-dependent uncertainty. These are shown in Fig. 1; red arrows show control force direction and magnitude. Note that the final position of the no-uncertainty trajectory is at the boundary of the terminal box constraint, resulting in the shortest possible trajectory and the least control effort. The trajectory with only control-dependent uncertainty terminates deeper into the terminal box constraint than the zero-uncertainty case, because the nominal trajectory must stand off from the feasible set boundary in order for the constraint to be robustly satisfied. Finally, the trajectory with both state- and control-dependent uncertainty stays near the r_x axis as long as possible before venturing up into the high-uncertainty region away from the r_x axis, to minimize uncertainty growth and retain feasibility.

B. Orbital Dynamics Example

The main motivation of this work is the development of algorithms for orbital spacecraft rendezvous. To demonstrate the suitability of our method to these problems, we assume linearized three-dimensional Clohessy-Wiltshire (CW) dynamics [24], which capture the relative motion of a chaser vehicle relative to a target vehicle in a circular orbit; we assume state-dependent uncertainty. With state $x = \begin{bmatrix} r_x & r_y & r_z & \dot{r}_x & \dot{r}_y & \dot{r}_z \end{bmatrix}^T$ (position components r_x, r_y, r_z have units of meters, velocity components $\dot{r}_x$, $\dot{r}_y$, $\dot{r}_z$ have units of m/s) and control $u = \begin{bmatrix} a_x & a_y & a_z \end{bmatrix}^T$ (units of $\mathrm{m/s^2}$), the continuous-time dynamics are:

$$\dot{x} = \begin{bmatrix} 0 & 0 & 0 & 1 & 0 & 0 \\ 0 & 0 & 0 & 0 & 1 & 0 \\ 0 & 0 & 0 & 0 & 0 & 1 \\ 3\omega^2 & 0 & 0 & 0 & -2\omega & 0 \\ 0 & 0 & 0 & -2\omega & 0 & 0 \\ 0 & 0 & -\omega^2 & 0 & 0 & 0 \end{bmatrix} x + \begin{bmatrix} \mathbf{0}_{3\times 3} \\ \mathbf{I}_{3\times 3} \end{bmatrix} u + K_x n_x$$

where

$$K_x = \begin{bmatrix} \mathcal{C}_3 & \mathbf{0}_{3\times 6} \\ \mathbf{0}_{3\times 6} & 0.1 \times \mathcal{C}_3 \end{bmatrix},$$

and ω is a mean-motion parameter that characterizes the speed of orbital motion. In our simulation we use $\omega = 0.3\ \mathrm{s^{-1}}$. Note that this is several orders of magnitude larger than is realistic for e.g. low Earth orbit; this was done simply to make the nontrivial dynamics more visible over the short time and distance span of the problem, and has no effect on the general applicability of the algorithm. We assume the following uncertainty bounds:

$$0 \preceq n_x \preceq 0.05 \times \|r - r_{lm}\|_2 \times \mathbf{1}_{12\times 1}$$

where r is the three-dimensional position component of the state (i.e., $r = \begin{bmatrix} r_x & r_y & r_z \end{bmatrix}^T$), and r_{lm} is the fixed position of a "landmark" in space, in this example located at $r_{lm} = \begin{bmatrix} 5 & -2 & 0 \end{bmatrix}^T$. This uncertainty bound represents the effect of using relative navigation techniques about the landmark, with state (and hence dynamics) uncertainty increasing with distance from the landmark. For example, the landmark could represent a space station which the chaser vehicle is scanning with lidar in order to determine its own state.

The constraints are as follows: initial state at the origin, final position in $r_x \in [9, 10]$, $r_y \in [-0.5, 0.5]$, $r_x \in [-0.5, 0.5]$, final velocity less than 0.1 m/s in all components, control magnitude less than 50 $\mathrm{m/s^2}$ in all components for all time. Our uncertainty function will tend to drive the trajectory toward the landmark in order to reduce uncertainty; in an actual relative navigation scenario, since the landmark is likely another spacecraft, we do not wish to approach in an uncontrolled manner. To simulate this, we impose an additional constraint that r_y be greater than -1 at all times; this keeps the vehicle some distance away from the landmark. We discretize the dynamics with zeroth-order hold (100 discretization points, 0.02 seconds apart) in order to solve the minimum-fuel trajectory optimization problem in `cvxpy`.

We first show the result of a trajectory optimization ignoring any uncertainty, for reference. The resulting trajectory in the r_x-r_y plane is shown in Fig. 2. This displays the standard phasing "hop" along the orbit track, with an initial thrust pulse to set the vehicle in motion, and a terminal pulse to stop the vehicle in the final bounding box. We also show in gray 1000 trajectories subject to the perturbations we ignored in planning the nominal trajectory; note that many of these violate the terminal box constraint. Compare this to the nominal trajectory generated with knowledge of the uncertainty, shown in Fig. 3. In order to prevent the uncertainty from growing until the final bounding constraint is no longer feasible, the vehicle dips down into the low-uncertainty region near the landmark, while respecting the keep-out plane constraint. Note that this plane constraint is also applied robustly: the nominal trajectory stands off some distance from the constraint. We also show 1000 perturbed trajectories in gray; note that all of them respect all constraints.

V. Conclusion

We have extended our previous duality-based robust optimization approach [1] to a much larger class of uncertainty sets, encompassing not only more general control-dependent uncertainty, but also now including state-dependent uncertainty as well. This broadens the relevance of our prior work to more sophisticated real-world error models, such as are often found when using relative navigation methods to plan vehicle rendezvous trajectories. We have demonstrated the

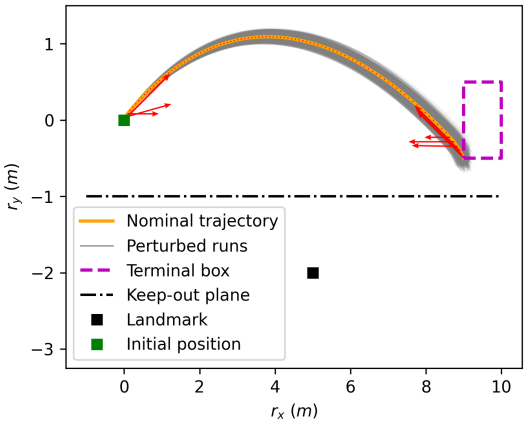

Fig. 2: CW dynamics, no uncertainty considered in planning. Nominal dynamics result in a feasible trajectory, but perturbed dynamics cause constraint violation.

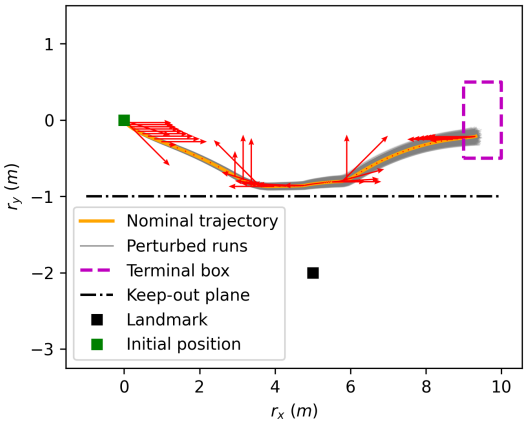

Fig. 3: CW dynamics, planning for uncertainty. All trajectories (nominal and perturbed) remain feasible.

practicality of our technique by the implementation of representative numerical examples. This technique is also readily adaptable to non-convex problems (including nonconvexity in the uncertainty bounding function $f(x^n, u)$) by the use of successive convex programming techniques such as in [25].

References

[1] O. Sheridan and B. Açıkmeşe, "Equivalent linear programming formulations for robust trajectory planning under input dependent uncertainties," in *2022 American Control Conference (ACC)*. IEEE, 2022, pp. 1873–1878.

[2] C. Gates, "A simplified model of midcourse maneuver execution errors," 1963.

[3] J. A. Christian and S. Cryan, "A survey of lidar technology and its use in spacecraft relative navigation," in *AIAA Guidance, Navigation, and Control (GNC) Conference*, 2013, p. 4641.

[4] R. C. Leishman, T. W. McLain, and R. W. Beard, "Relative navigation approach for vision-based aerial gps-denied navigation," *Journal of Intelligent & Robotic Systems*, vol. 74, pp. 97–111, 2014.

[5] J. S. Shamma and K.-Y. Tu, "Set-valued observers and optimal disturbance rejection," *IEEE Transactions on Automatic Control*, vol. 44, no. 2, pp. 253–264, 1999.

[6] A. W. Berning, A. Girard, I. Kolmanovsky, and S. N. D'Souza, "Rapid uncertainty propagation and chance-constrained path planning for small unmanned aerial vehicles," *Advanced Control for Applications: Engineering and Industrial Systems*, vol. 2, no. 1, p. e23, 2020.

[7] H. Zhu and J. Alonso-Mora, "B-uavc: Buffered uncertainty-aware voronoi cells for probabilistic multi-robot collision avoidance," in *2019 international symposium on multi-robot and multi-agent systems (MRS)*. IEEE, 2019, pp. 162–168.

[8] D. Malyuta, B. Açikmeşe, and M. Cacan, "Robust model predictive control for linear systems with state and input dependent uncertainties," in *2019 American Control Conference (ACC)*. IEEE, 2019, pp. 1145–1151.

[9] G. Pin, D. M. Raimondo, L. Magni, and T. Parisini, "Robust model predictive control of nonlinear systems with bounded and state-dependent uncertainties," *IEEE Transactions on automatic control*, vol. 54, no. 7, pp. 1681–1687, 2009.

[10] R. Soloperto, M. A. Müller, S. Trimpe, and F. Allgöwer, "Learning-based robust model predictive control with state-dependent uncertainty," *IFAC-PapersOnLine*, vol. 51, no. 20, pp. 442–447, 2018.

[11] X. Wang, L. Yang, Y. Sun, and K. Deng, "Adaptive model predictive control of nonlinear systems with state-dependent uncertainties," *International Journal of Robust and Nonlinear Control*, vol. 27, no. 17, pp. 4138–4153, 2017.

[12] S. Boyd, S. P. Boyd, and L. Vandenberghe, *Convex optimization*. Cambridge university press, 2004.

[13] F. Blanchini, "Set invariance in control," *Automatica*, vol. 35, no. 11, pp. 1747–1767, 1999.

[14] F. Blanchini and S. Miani, *Set-theoretic methods in control*. Springer, 2008.

[15] S. V. Rakovic and M. Baric, "Parameterized robust control invariant sets for linear systems: Theoretical advances and computational remarks," *IEEE Transactions on Automatic Control*, vol. 55, no. 7, pp. 1599–1614, 2010.

[16] A. Weiss, C. Petersen, M. Baldwin, R. S. Erwin, and I. Kolmanovsky, "Safe positively invariant sets for spacecraft obstacle avoidance," *Journal of Guidance, Control, and Dynamics*, vol. 38, no. 4, pp. 720–732, 2015.

[17] B. Açıkmeşe, N. Demir, and M. W. Harris, "Convex necessary and sufficient conditions for density safety constraints in markov chain synthesis," *IEEE Transactions on Automatic Control*, vol. 60, no. 10, pp. 2813–2818, 2015.

[18] M. El Chamie, Y. Yu, B. Açıkmeşe, and M. Ono, "Controlled markov processes with safety state constraints," *IEEE Transactions on Automatic Control*, vol. 64, no. 3, pp. 1003–1018, 2018.

[19] E. D. Andersen and K. D. Andersen, "The mosek interior point optimizer for linear programming: an implementation of the homogeneous algorithm," *High performance optimization*, pp. 197–232, 2000.

[20] A. Domahidi, E. Chu, and S. Boyd, "Ecos: An socp solver for embedded systems," in *2013 European control conference (ECC)*. IEEE, 2013, pp. 3071–3076.

[21] Y. Yu, P. Elango, U. Topcu, and B. Açıkmeşe, "Proportional–integral projected gradient method for conic optimization," *Automatica*, vol. 142, p. 110359, 2022.

[22] D. Malyuta, T. Reynolds, M. Szmuk, M. Mesbahi, B. Acikmese, and J. M. Carson, "Discretization performance and accuracy analysis for the rocket powered descent guidance problem," in *AIAA Scitech 2019 Forum*, 2019, p. 0925.

[23] S. Diamond and S. Boyd, "Cvxpy: A python-embedded modeling language for convex optimization," *The Journal of Machine Learning Research*, vol. 17, no. 1, pp. 2909–2913, 2016.

[24] W. Clohessy and R. Wiltshire, "Terminal guidance system for satellite rendezvous," *Journal of the Aerospace Sciences*, vol. 27, no. 9, pp. 653–658, 1960.

[25] D. Malyuta, T. P. Reynolds, M. Szmuk, T. Lew, R. Bonalli, M. Pavone, and B. Açıkmeşe, "Convex optimization for trajectory generation: A tutorial on generating dynamically feasible trajectories reliably and efficiently," *IEEE Control Systems Magazine*, vol. 42, no. 5, pp. 40–113, 2022.